Model for Sr–Cs–Ca–Mg–Na Ion-Exchange Uptake Kinetics on Chabazite

Susan M. DePaoli
Oak Ridge National Laboratory, Oak Ridge, TN 37831

Joseph J. Perona
Dept. of Chemical Engineering, University of Tennessee, Knoxville, TN 37996

Many nuclear facilities throughout the world must separate strontium-90 and cesium-137 from natural waters containing calcium, magnesium, and sodium. Our research showed that chabazite, a zeolite with a hexagonal ring structure, is cost-effective for this purpose. A batch kinetic uptake model for this five-component ion-exchange system was developed and tested against experimental data. The pore-diffusion model of Yao and Tien is used with the equilibrium model of Perona. The resulting model is fast and stable, and represents the experimental data well.

Introduction

Many nuclear facilities throughout the world must process groundwaters and wastewaters for the removal of strontium-90 and cesium-137. These waters usually contain calcium, magnesium, and sodium in concentrations many orders of magnitude larger than the radioactive species. Typical cation and anion concentrations in wastewater from Oak Ridge National Laboratory (ORNL) are shown in Table 1. Treatability studies by Robinson and Begovich (1991) support the use of chabazite zeolite as the most cost-effective means of separation of the radioactive species from the ORNL wastewater. Chabazite is relatively inexpensive, and secondary waste generation for this treatment process would constitute a spent zeolite that would be disposed of as a solid waste.

Physical properties of the chabazite zeolite pellet used in a study by Robinson et al. (1994) are shown in Table 2. These researchers worked with both zeolite crystals (Ionsiv IE-90) and zeolite pellets (Ionsiv IE-96), which are the crystals held together with a clay binder to form a larger particle. This present study deals only with the pellet form of the zeolite, IE-96, since that is the form of zeolite to be used in further fixed-bed studies.

The experimental data modeled in this article are taken from the study by Robinson and coworkers (1994). In the referenced study, multicomponent equilibrium was estimated using a modified Dubinin–Polyani model. Kinetic uptake data were modeled based on solid diffusion and combinations of macropore and micropore diffusion, and the mathematical model was solved by orthogonal collocation. In the present article a thermodynamic equilibrium model developed by Perona (1993) for the same system is used in combination with an approximate solution to the pore-diffusion model presented by Yao and Tien (1993). Data for two five-component uptake experiments (SK-24 and SK-34) were used, having total cationic concentrations of 1.58 meq/L and 6.29 meq/L. The approximate solution of Yao and Tien (1993) is based on assumptions that allow the partial differential equations to be reduced to ordinary differential equations. The pore-diffusion model was found to require less computer time and to be more stable for this multicomponent system than the orthogonal collocation model.

Model Development

Diffusion of a species prior to ion exchange takes place in two regions: (1) the solution outside the particle, and (2) within the particle. The transport resistance outside the par-

Table 1. Typical Cation/Anion Concentrations in ORNL Wastewater

Species	Conc. (N)	Species	Conc. (N)
Ca^{2+}	2.0×10^{-3}	HCO_3^-	1.5×10^{-3}
Mg^{2+}	6.6×10^{-4}	SO_4^{2-}	4.8×10^{-4}
Na^+	2.2×10^{-4}	Cl^-	2.8×10^{-4}
$^{90}Sr^{2+}$	1.7×10^{-11}	NO_3^-	1.8×10^{-4}
$^{137}Cs^+$	9.1×10^{-13}	CO_3^{2-}	2.3×10^{-4}

Correspondence concerning this article should be addressed to S. M. DePaoli.

Table 2. Physical Properties of Chabazite Zeolite IE-96 Pellets*

Property	Units	Value
Bulk density	g/cm^3	1.39
Real density	g/cm^3	2.05
Porosity	cm^3 pore/cm^3 total particle	0.32
Avg. particle radius	cm	0.02725
Max. pore radius	cm	5.0
Surface area	m^2/g	360
Moisture content	%	6.9–7.9
Avg. composition	Na_2O%	7.9
	K_2O%	1.0
	MgO%	0.8
	CaO%	1.2
	BaO%	0.1
	SiO_2%	67.4
	Al_2O_3%	17.3
	FeO%	4.0
	TiO%	0.2

*Robinson et al. (1994).

ticle occurs in the film surrounding the particle. For a batch-stirred contactor, the bulk liquid is assumed to be well mixed, and the concentration of species *i* in the bulk liquid phase is assumed constant at any time throughout the contactor.

Diffusion of species *i* within the particle is much more complicated and may occur by various mechanisms—solid diffusion, pore diffusion, surface diffusion, or a combination of these (Ruthven, 1984). Mass transfer within a porous pellet (such as chabazite zeolite) can take place at several levels, and can be modeled more simplistically by assuming a homogeneous pellet, which requires a single solid-phase diffusion coefficient (the homogeneous-diffusion model). This assumption does not work well for zeolite pellets composed of crystals and binder. Zeolite crystals would be expected to be much more amenable to this type of model. Robinson et al. (1994) showed this to be the case. Their homogeneous-diffusion model satisfactorily modeled single-crystal uptake rates of single solutes, but failed to model single or multicomponent uptake by zeolite pellets.

The next step in complexity would be to assume diffusion through the pores (pore diffusion) or diffusion along the surface of the pores (surface diffusion) as the rate-limiting mechanism. In pore diffusion, the liquid in the pores is considered to be in equilibrium with the adsorbed solid phase. The pore-diffusion model is considered more accurate (as opposed to a surface-diffusion model) if, in a multicomponent system, some species are more strongly adsorbed than other species. Surface-diffusion modeling is usually used when weakly adsorbed species are not present (Friedman, 1984). A combination of pore and surface diffusion is sometimes referred to as heterogeneous diffusion (e.g., Fettig and Sontheimer, 1987; Merk et al., 1981).

A different meaning for "heterogeneous diffusion" is often used for a composite solid, in which mass transfer occurs (a) in the pores of the pellet (macropore diffusion by pore and/or surface diffusion), and (b) in the solid crystals (micropore diffusion). Both of these diffusional fluxes are taken into account in the heterogeneous-diffusion model (Fritz et al., 1981). These mechanisms (macropore and micropore diffusion) can be assumed to occur in parallel or in series with each other (Robinson et al., 1994). The heterogeneous structure of the zeolites makes the heterogeneous-diffusion models, which assume pore and/or surface macropore diffusion and solid, micropore internal resistances most realistic; however, they are also much more complicated (Ruthven, 1984). Robinson et al. (1994) modeled the multicomponent system under study in this article using macropore–micropore diffusion models in parallel and series.

Many authors have solved adsorption problems assuming a parabolic concentration profile within the particle (e.g., Do and Rice, 1986). This assumption simplifies the mathematics by allowing the PDEs describing the adsorption processes to be reduced to ODEs. Yao and Tien (1993) assumed a parabolic intraparticle concentration profile for separate cases of pore- and surface-diffusion control. In their solutions, a "concentration layer" is defined within the particle in which the parabolic concentration profile is assumed. From the center of the particle to this "layer" the concentration is assumed to be the initial concentration within the pores (usually zero). The PDEs describing pore (surface) diffusion can then be reduced to ODEs, with the coefficients of the parabolic profile and the width of the boundary layer determined as functions of the various concentrations.

Pore diffusion is usually assumed to be the rate-controlling intraparticle process (over surface diffusion) if, in a multicomponent system, some species are more strongly adsorbed than other species (Friedman, 1984) as is the case here. Robinson and coworkers (1994) showed that chabazite zeolite adsorbs cesium most strongly, the order of selectivity being Cs > Sr > Ca > Mg > Na. In addition to this consideration, the surface-diffusion coefficients were estimated by Robinson to be on the order of 10^{-9} cm^2/s compared with effective pore-diffusion coefficients on the order of 10^{-5} cm^2/s, also supporting the dominance of pore diffusion (since these intraparticle mechanisms occur in parallel).

Diffusional Model

The pore-diffusion approximate solution presented by Yao and Tien (1993) was chosen to represent the kinetics for the present five-component system, since their results showed excellent agreement with orthogonal collocation solutions, and computer times would be shorter using the less complex model compared to the heterogeneous model of Robinson et al. (1994). In their article, Yao and Tien (1993) develop the pore-diffusion model for a single component. For a multicomponent system, the intraparticle mass balance for pore diffusion of species *i* would be

$$\epsilon_p \frac{\partial c_{pi}}{\partial t} + \frac{\partial q_i}{\partial t} = \frac{1}{r^2}\frac{\partial}{\partial r}\left(r^2 \epsilon_p D_{pi} \frac{\partial c_{pi}}{\partial r}\right), \tag{1}$$

where

ϵ_p = porosity of adsorbent, mL pore/mL particle
c_{pi} = pore concentration of species *i*, meq/mL pore
D_{pi} = overall pore-diffusion coefficient, cm^2/s
q_i = adsorbed concentration of species *i*, meq/mL particle
r = radial position, cm
t = time, s

The effective diffusivity for adsorbate *i*, D_{ei}, is defined as:

$$D_{ei} \equiv \epsilon_p D_{pi}. \tag{2}$$

Boundary and initial conditions for the preceding case, adsorption of n, i-species into a spherical particle are:

$$\text{at} \quad t = 0 \qquad c_{pi} = c_{pi_0}, \tag{3}$$

$$\text{at} \quad r = R_p \qquad D_{ei}\frac{\partial c_{pi}}{\partial r}\bigg|_{r=R_p} = k_{fi}(c_{bi} - c_{pi}|_{r=R_p}) \tag{4}$$

and

$$\text{at} \quad r = 0 \qquad \frac{\partial c_{pi}}{\partial r} = 0, \tag{5}$$

where

c_{bi} = bulk-liquid concentration of species i, meq/mL
k_{fi} = film mass-transfer coefficient for species i, cm/s
R_p = particle radius, cm

The equations are then written in terms of the following dimensionless variables:

$$\tau \equiv \frac{D_{ei}t}{R_p^2} \qquad \text{and} \qquad x \equiv \frac{r}{R_p}, \tag{6}$$

and the dimensionless Biot number for component i,

$$Bi_i \equiv \frac{k_{fi}R_p}{D_{ei}}. \tag{7}$$

Assuming a constant diffusivity, the mass balance for pore diffusion becomes:

$$(\epsilon_p + f'(c_{pi}))\frac{\partial c_{pi}}{\partial \tau} = \frac{1}{x^2}\frac{\partial}{\partial x}\left(x^2\frac{\partial c_{pi}}{\partial x}\right), \tag{8}$$

where $f(c_{pi})$ is the equilibrium relationship.

For a multicomponent system, the equilibrium adsorbed-phase concentration for species i (with $i = 1$) is dependent on the local concentration of all adsorbable components (Ruthven, 1984):

$$f'(c_{p1}) = \frac{dq_1}{dc_{p1}} = \frac{\partial q_1}{\partial c_{p1}}\bigg|_{c_{p2}\cdots c_{pn}} + \frac{\partial q_1}{\partial c_{p2}}\frac{\partial c_{p2}}{\partial c_{p1}}\bigg|_{c_{p1},c_{p3}\cdots c_{pn}} + \cdots + \frac{\partial q_1}{\partial c_{pn}}\frac{\partial c_{pn}}{\partial c_{p1}}\bigg|_{c_{p1}\cdots c_{pn-1}}. \tag{9}$$

Assuming, at any time, τ,

$$C_{p\,\mathrm{tot}} = c_{p1} + c_{p2} + \cdots + c_{pn} \tag{10}$$

and assuming constant total pore concentration, $C_{p\,\mathrm{tot}}$, Eq. 9 reduces to:

$$f'(c_{p1}) = \frac{dq_1}{dc_{p1}} = \frac{\partial q_1}{\partial c_{p1}}\bigg|_{c_{p2}\cdots c_{pn}} - \frac{\partial q_1}{\partial c_{p2}}\bigg|_{c_{p1},c_{p3}\cdots c_{pn}} - \cdots - \frac{\partial q_1}{\partial c_{pn}}\bigg|_{c_{p1}\cdots c_{pn-1}}, \tag{11}$$

Yao and Tien (1993) define a parabolic concentration layer within the particle of width δ. They represent the pore concentration of species i as

$$\begin{aligned} c_{pi} &= a_i + b_i x + c_i x^2 \quad &&\text{for} \quad 1 - \delta \le x \le 1 \\ c_{pi} &= c_{pi_0} &&\text{for} \quad 0 \le x \le 1 - \delta. \end{aligned} \tag{12}$$

The reader is referred to Yao and Tien (1993) for the details that result in their approximate solution to the pore-diffusion model:

$$\frac{\partial c_{pi}}{\partial x}\bigg|_{x=1} = \frac{2(c_{si} - c_{pi_0})\left(c_{si} - c_{pi_0} - \dfrac{\bar{c}_{pi} - c_{pi_0}}{2}\right)}{\bar{c}_{pi} - c_{pi_0}}, \tag{13}$$

where c_{si} is the surface concentration of species i and the overbar denotes the average value.

Yao and Tien introduce an approximation:

$$\bar{f}(c_{pi}) \approx f(\bar{c}_{pi}), \tag{14}$$

which is exact for a linear isotherm. The deviation of this assumption from real behavior depends on the extent of nonlinearity of the isotherm. The final equations for Yao and Tien's Model I for intracrystalline pore diffusion are

$$(\epsilon_p + f'(\bar{c}_{pi}))\frac{d\bar{c}_{pi}}{d\tau} = 6\left[\frac{c_{si} - c_{pi_0}}{\bar{c}_{pi} - c_{pi_0}} + \frac{1}{2}\right](c_{si} - \bar{c}_{pi}) \tag{15}$$

$$Bi_i(c_{bi} - c_{si}) = 2\left[\frac{c_{si} - c_{pi_0}}{\bar{c}_{pi} - c_{pi_0}} + \frac{1}{2}\right](c_{si} - \bar{c}_{pi}). \tag{16}$$

These two equations are combined to give:

$$\frac{d\bar{c}_{pi}}{d\tau} = \frac{3Bi_i(c_{bi} - c_{si})}{(\epsilon_p + f'(\bar{c}_{pi}))}, \tag{17}$$

which can be solved numerically for each component. In this study, Eq. 17 was solved using a fourth-order Runge–Kutta routine.

The values for c_{bi} and c_{si} in the preceding equation are found by writing an overall mass balance:

$$V_f(c_{bi_0} - c_{bi}) = V_s(\epsilon_p\bar{c}_{pi} + \bar{q}_i) \tag{18}$$

and from Eq. 16, assuming $c_{pi_0} = 0$ at $\tau = 0$:

$$2\left(\frac{c_{si}}{\bar{c}_{pi}} + \frac{1}{2}\right)(c_{si} - \bar{c}_{pi}) = Bi_i(c_{bi} - c_{si}), \tag{19}$$

which can be solved to obtain c_{si}.

Equilibrium Model

The adsorption-equilibrium model for the multicomponent system Cs–Sr–Ca–Mg–Na was developed by Perona (1993) based on fundamental thermodynamic relationships. Following is a brief discussion of the theory involved.

An ion-exchange reaction between a species in solution, A, and the ion in the solid phase, $\boldsymbol{B}$, can be expressed as

$$bA^{+a} + a\boldsymbol{B}^{+b} \leftrightarrows b\boldsymbol{A}^{+a} + aB^{+b}.$$

The equilibrium constant, K_{A-B} for the preceding reaction is written:

$$K_{A-B} = \left(\frac{\underline{\gamma}_A y_A}{\gamma_A c_A} \right)^b \left(\frac{\gamma_B c_B}{\underline{\gamma}_B y_B} \right)^a , \tag{20}$$

where

y_i = equivalents fraction of i in the solid phase
c_i = normality of i in the liquid phase, meq/mL
γ_i = activity coefficient of i in the liquid phase
$\underline{\gamma}_i$ = activity coefficient of i in the solid phase

In Perona's model, the Pitzer equation is used to calculate the liquid-phase activity coefficients, and the Wilson equation is used to calculate solid-phase activity coefficients. This relationship relates the solid-phase fraction to the solid-phase activity coefficients, and is based on the Gibbs–Duhem equation. Wilson's equation for a multicomponent system is written:

$$\ln \gamma_i = 1 - \ln\left(\sum_{j=1}^{m} y_j \Lambda_{ij} \right) - \sum_{k=1}^{m} \left(\frac{y_k \Lambda_{ki}}{\sum_{j=1}^{m} y_j \Lambda_{kj}} \right), \tag{21}$$

where the Λ terms are the interaction parameters that are found by fitting experimental binary data for the multiple pairs (where all $\Lambda_{jj} = 1$). In turn, for the multicomponent system these binary interaction parameters are used in this same Wilson equation. Through the use of the equilibrium relationship in Eq. 10, the Pitzer and the Wilson equations, and binary pair equilibrium data, the multicomponent isotherms are predicted. These equilibrium expressions can then be used in the rate equations to completely model the kinetics of the system.

The role of the equilibrium model within the kinetic model is shown in Eq. 8. The calculation of the derivative of the equilibrium model, $f'(\bar{c}_{pi})$, for equilibrium models such as the Langmuir or Freundlich models, is relatively straightforward. Both are simple equations where the average solid-phase adsorbed concentration is given as a function of the average liquid concentration for a single species, and these derivatives can be expressed as a single function. For this thermodynamic model, the concentration of species i in the solid phase, in equilibrium with the liquid concentration of all n-components, requires an iterative approach. A change in the liquid concentration of a single component would be expected to elicit a change in the loading of all components. Equation 11 demonstrates this interdependence for a multicomponent system. A finite difference technique was used to calculate the change in the solid loading of species i for small step changes, ξ, in each solute (average) pore concentration while holding all other average pore concentrations constant (Lapidus and Pinder, 1982):

$$\left.\frac{\partial q_i}{\partial \bar{c}_{pi}}\right|_{\bar{c}_{pi+1,\ldots,n}} = \frac{q_i|_{\bar{c}_{pi}+\xi} + q_i|_{\bar{c}_{pi}-\xi}}{2\xi}. \tag{22}$$

The total derivative for a solute was then calculated as a combination of the partial derivatives with respect to the change in each liquid-phase solute as in Eq. 11.

An additional assumption was necessary in order to utilize the Perona model. In order to predict solid loading, the equilibrium model requires the liquid concentrations of all exchanging components, including sodium. The initial sodium concentration in the pores was assumed to be equal to the bulk-liquid cationic concentration, representing no net charge difference (or osmotic pressure difference) between bulk and pore liquids. Assuming electroneutrality, the total pore concentration in terms of total positive charges was considered to be constant for all time. Thus the iterative technique for converging upon equilibrium solution concentrations included the additional constraint that the sodium concentration equal the total concentration less the concentrations of the other species.

Determination of Constants

The defining equation for the film mass-transfer coefficient, k_{fi} (cm/s), for a spherical particle is written (Ruthven, 1984):

$$m_t = \frac{3k_{fi}}{R_p}(c_{bi} - c_{si}). \tag{23}$$

Many empirical relationships exist for the calculation of film mass-transfer coefficients in batch reactors (e.g., Ruthven, 1984; Cornell et al., 1986; Smith and Weber, 1988). Most of these relationships involve the power input to the stirrer and the physical properties of the solutions. These correlations do not, however, account for the surface topography and roughness of an adsorbent that can impact the film mass-transfer coefficient (Smith and Weber, 1988).

Film mass-transfer coefficients can also be determined from experimental data by fitting the initial slope of the transient uptake (e.g., Fettig and Sontheimer, 1987; Weber and Wang, 1987; Smith and Weber, 1988; Robinson et al., 1994). Initial experimental points can be assumed to be unaffected by intraparticle mass transfer, and thus the film mass-transfer coefficient can be found by

$$\frac{V_f}{V_s}\frac{\partial c_{bi}}{\partial t} + \frac{3}{R_p}k_{fi}(c_{bi} - c_{si}) = 0 \tag{24}$$

assuming c_s is negligible as t approaches zero. For multicomponent systems, film mass-transfer coefficients must be determined experimentally, because correlations do not account for the decreased rates due to component interactions (Smith and Weber, 1988).

Table 3. Film Mass-Transfer Coefficients for Binary and Multicomponent Systems

	Binary System		Multicomponent
Component	Range of k_f (cm/s) from Correlations*	k_{fi} (cm/s) Experimental	k_{fi} (cm/s) Experimental
Film mass-transfer coefficients found by fitting the initial experimental data with the pore-diffusion model for binary cases and multicomponent cases for experimental data run (SK-34, total cationic concentration 6.29 meq/L).			
Strontium	0.001–0.018	0.009	0.002
Cesium	0.0015–0.024	0.021	0.004
Calcium	0.0011–0.018	0.006	0.0018
Magnesium	0.001–0.017	0.004	0.0025
Film mass-transfer coefficients found by fitting the initial experimental data for the lower concentration multicomponent run (SK-24, total cationic concentration 1.58 meq/L) with the pore-diffusion model.			
Strontium			0.01
Cesium			0.006
Calcium			0.006
Magnesium			0.004

*As calculated by Robinson et al. (1994).

Film mass-transfer coefficients were determined by Robinson et al. (1994) for binary systems using various semiempirical correlations and also by fitting the experimental data. The correlations included the Treybal, Gilliland–Sherwood, Froessling, and Ranz and Marshall correlations. For comparison purposes, the binary-film mass-transfer coefficients obtained by Robinson using the correlations are shown in Table 3 along with the values obtained by fitting binary data with the Yao and Tien pore-diffusion model. Those k_{fi} values found by modeling the experimental data fall well within the ranges predicted by the correlations. The multicomponent film mass-transfer coefficients, which were found by fitting the data, are also shown in Table 3. The multicomponent film mass-transfer coefficients were consistently lower than the corresponding binary coefficients.

For a multicomponent system, individual film mass-transfer coefficients would be expected to be lower than those for a binary system (Smith and Weber, 1988). This is explained by the competition present with multiple diffusing and counterdiffusing species. As the concentrations of the species decrease in a multicomponent situation, one would expect the film mass-transfer coefficients to approach the values estimated for the single components. This was demonstrated in modeling the more dilute multicomponent experimental data (SK-24) for which slightly higher values for k_f were required to fit the initial uptake curves (see Table 3).

Effective pore-diffusion coefficients for the exchanging species in this study are given in Table 4. With the exception of the diffusion coefficient for calcium, these are the diffusion coefficients that were determined by Robinson and coworkers (1994) through fitting the orthogonal collocation model. The diffusion coefficient for calcium was decreased, providing an improved fit to the experimental data.

Table 4. Effective Pore Diffusivities for the Sr–Cs–Ca–Mg–Na Multicomponent System

Component	$D_{p,eff}$ (cm^2/s)
Strontium	5.0×10^{-5}
Cesium	1.5×10^{-4}
Calcium	1.0×10^{-5}
Magnesium	1.0×10^{-3}

The dimensionless Biot number (defined in Eq. 7) is the ratio of the external-phase mass-transfer rate to the intraparticle-phase mass-transfer rate. As the Biot number increases (generally over 30), the intraparticle mass-transfer rate is reduced and thus controls the overall exchange rate, while a smaller Biot number (< 0.5) signals an external (film) mass-transfer rate-controlled process (Crittenden et al., 1980; Friedman, 1984). For this system Biot numbers for each component—in both binary exchange and multicomponent exchange—are about 2.5. This value supports the significance of both mass-transfer resistances.

The maximum loading of the IE-96 chabazite zeolite was found by Robinson and coworkers (1994) to be 3.2 meq/g in the presence of cesium, and 2.8 meq/g without cesium in the solution. Researchers Dyer and Keir (1989) found the maximum loading of chabazite zeolite IE-96 to be 2.22 meq/g. An intermediate value of 2.6 meq/g was used in this study, as it predicted the loading for all cases (binary and multicomponent) with the least error.

Results and Discussion

Uptake curves for binary and multicomponent systems were predicted using Yao and Tien's (1993) approximate solution to the pore-diffusion model. The first set of kinetic data, SK-34, was run at higher initial experimental concentrations for each component (on the order of 10^{-3} meq/mL). Figures 1 through 4 show the experimental values for the transient uptake from solution of strontium, cesium, calcium, and magnesium vs. that predicted by the multicomponent model. The uptake of each component was predicted quite well, with percent variances of 1.7%, 3.3%, 3.3%, and 2.6% for strontium, cesium, calcium, and magnesium, respectively.

The variance was calculated by

$$\sigma = \left[\frac{1}{n} \sum_{i=1}^{n} \left(\frac{\text{experimental} - \text{theoretical}}{\text{experimental}} \right)^2 \right]^{0.5}. \tag{25}$$

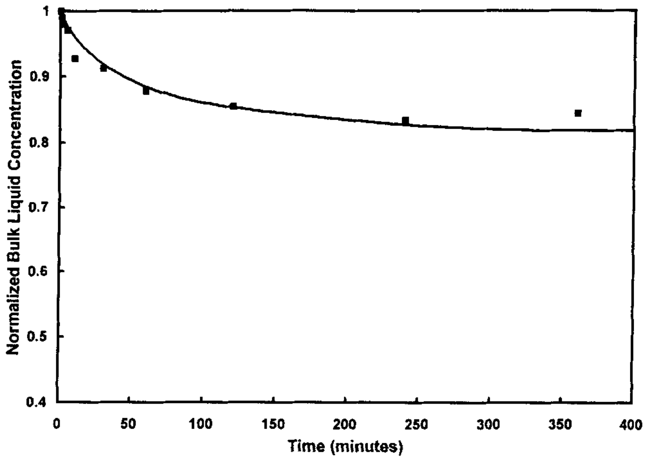

Figure 1. Strontium uptake on chabazite zeolite in Sr–Cs–Ca–Mg–Na multicomponent ion exchange for experimental run SK-34.

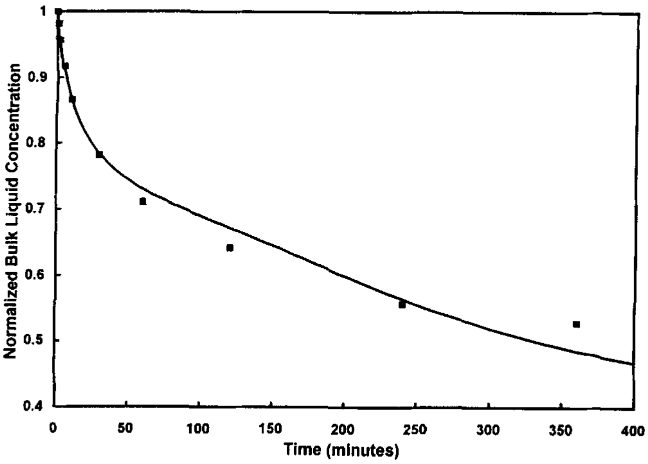

Figure 2. Cesium uptake on chabazite zeolite in Sr–Cs–Ca–Mg–Na multicomponent ion exchange for experimental run SK-34.

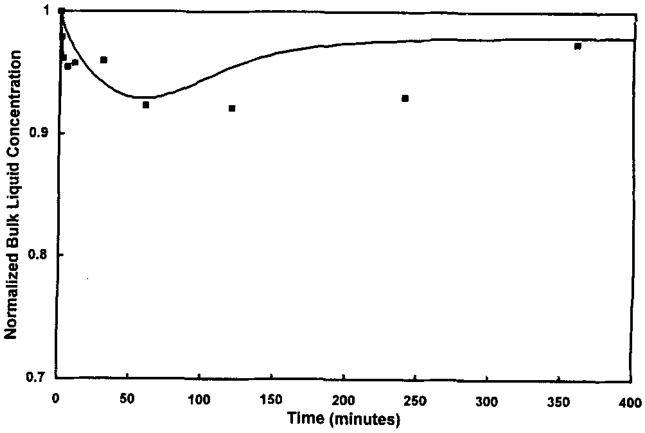

Figure 4. Magnesium uptake on chabazite zeolite in Sr–Cs–Ca–Mg–Na multicomponent ion exchange for experimental run SK-34.

Film mass-transfer coefficients were found by fitting the initial experimental uptake curve with the model. Table 3 contains the values as calculated by this technique. Multicomponent-film mass-transfer coefficients are somewhat lower than those calculated for binary systems, as expected due to the competition resulting from multiple species diffusing and counterdiffusing through the film layer (Smith and Weber, 1988).

Effective pore diffusivities used in the model are listed in Table 4. These values agree with those obtained by Robinson and coworkers (1994) by fitting experimental data with a heterogeneous-series-diffusion model, with the exception of calcium. The uptake curves were fairly insensitive to effective diffusivity, requiring about an order of magnitude change for any species to have a significant effect. The current model fit the experimental uptake curves for run SK-34 better when the value of diffusivity of calcium used by Robinson was decreased by a factor of 6, giving the number in Table 4.

A second set of experimental kinetic uptake data (run SK-24 having an order of magnitude lower initial concentration for each component than the previous SK-34 data run) was predicted (Figures 5 through 8). Variances of 14.8%, 34.2%, 6.9%, and 4.6% for strontium, cesium, calcium, and magnesium uptake, respectively, were calculated for this run.

Film mass-transfer coefficients were adjusted to fit the initial slope of the uptake curve, as was done for the previous multicomponent experimental data set. Since the total concentration (and the concentration of each species) was lower in the SK-24 experimental data than the SK-34 data, the film mass-transfer coefficients would be expected to be higher due to the decreased diffusion and counterdiffusion of competing and like species. The individual film mass-transfer coefficients approached the values obtained in the binary exchanges, as would be expected. Diffusion coefficients were not changed from the previous run.

Magnesium, the least strongly adsorbed species, experiences a minimum in both experimental runs. This phenomenon—a result of the magnesium that is quickly adsorbed being displaced by the more strongly (and less quickly)

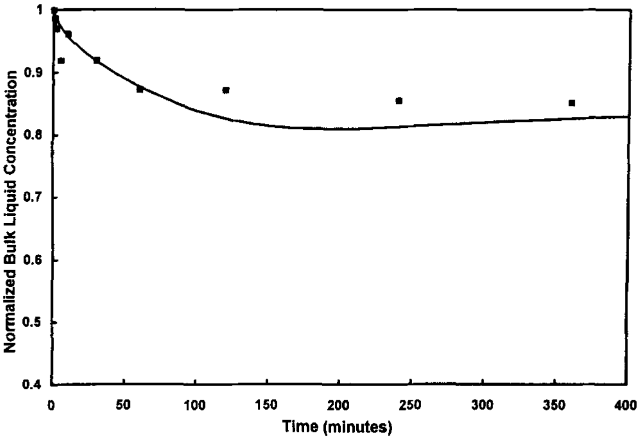

Figure 3. Calcium uptake on chabazite zeolite in Sr–Cs–Ca–Mg–Na multicomponent ion exchange for experimental run SK-34.

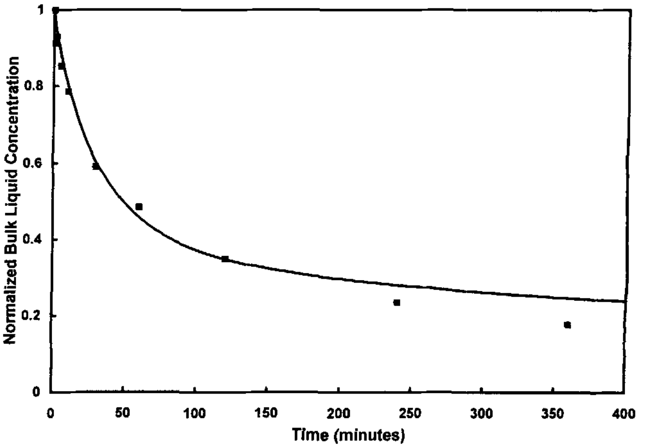

Figure 5. Strontium uptake on chabazite zeolite in Sr–Cs–Ca–Mg–Na multicomponent ion exchange for experimental run SK-24.

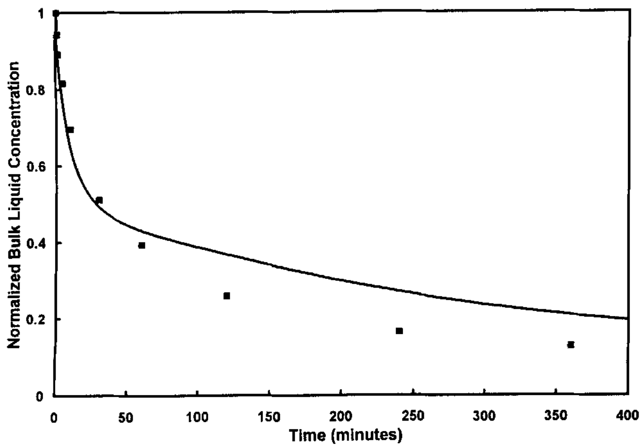

Figure 6. Cesium uptake on chabazite zeolite in Sr-Cs-Ca-Mg-Na multicomponent ion exchange for experimental run SK-24.

adsorbed species—is appropriately predicted by the model.

The results from fitting both experimental data sets support the fact that film mass transfer is a significant rate-determining step in this system, as is the intraparticle diffusion, which is suitably modeled assuming macropore diffusion. The Perona equilibrium model accurately modeled the multicomponent uptake for both experimental cases.

Conclusions

An approximate solution to the pore-diffusion model—as presented by Yao and Tien (1993) for calculating transient uptake in a spherical porous particle, assuming external film mass transfer and intraparticle macropore diffusion—was employed with a thermodynamic equilibrium model (Perona, 1993) to accurately predict uptake rates in multicomponent ion exchange on chabazite zeolite. Film mass-transfer coefficients on the order of 10^{-3} cm/s were obtained; these values agree well with values reported in the literature. The dimensionless Biot numbers were estimated to be approximately 2.5 for the exchanging cations, indicating that intraparticle diffusion and external diffusion are both significant in controlling the rate of exchange. Variations in the effective pore diffusivities for the binary pairs altered the uptake curves somewhat; however, film mass-transfer coefficient variations more significantly affected the uptake curves. Model predictions employing effective pore diffusivities on the order of 10^{-5} cm^2/s matched the experimental data accurately. These values for effective diffusivities agree well with those reported in the literature.

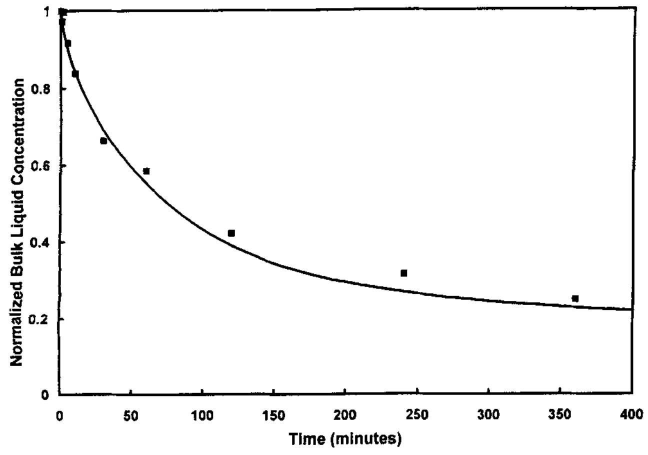

Figure 7. Calcium uptake on chabazite zeolite in Sr-Cs-Ca-Mg-Na multicomponent ion exchange for experimental run SK-24.

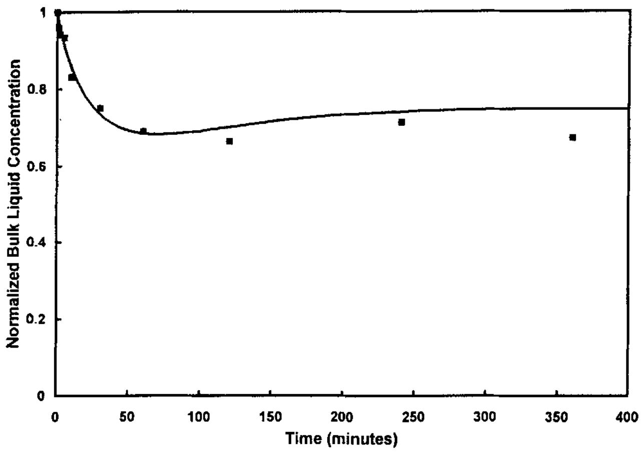

Figure 8. Magnesium uptake on chabazite zeolite in Sr-Cs-Ca-Mg-Na multicomponent ion exchange for experimental run SK-24.

Notation

m_t = uptake rate, mol/mL·s
V_f = volume of liquid phase, mL
V_s = volume of solid phase, mL

Literature Cited

Cornel, P., H. Sontheimer, R. S. Summers, and P. V. Roberts, "Sorption of Dissolved Organics from Aqueous Solution by Polystyrene Resins—II External and Internal Mass Transfer," *Chem. Eng. Sci.*, **41**(7), 1801 (1986).

Crittenden, J. C., B. W. C. Wong, W. E. Thacker, and R. L. Hinrichs, "Mathematical Model of Sequential Loading in Fixed Bed Adsorbers," *J. Water Pollut. Cont. Fed.*, **52**(11), 2780 (1980).

Do, D. D., and R. G. Rice, "Validity of the Parabolic Profile Assumption in Adsorption Studies," *AIChE J.*, **32**, 149 (1986).

Dyer, A., and D. Keir, "Ion Exchange and pH Tolerance in Molecular Sieve Zeolites," *J. Radioanal. Nucl. Chem. Artic.*, **132**(2), 423 (1989).

Fettig, J., and H. Sontheimer, "Kinetics of Adsorption on Activated Carbon: I. Single Solute Systems," *J. Environ. Eng.*, **113**(4), 764 (1987).

Friedman, G., "Mathematical Modeling of Multicomponent Adsorption in Batch and Fixed-Bed Reactors," MS Thesis, Michigan Technological Univ., Houghton (1984).

Fritz, W., W. Merk, and E. U. Schlunder, "Competitive Adsorption of Two Dissolved Organics onto Activated Carbon-II," *Chem. Eng. Sci.*, **36**, 731 (1981).

Lapidus, L., and G. F. Pinder, *Numerical Solution of Partial Differential Equations in Science and Engineering*, Wiley, New York (1982).

Merk, W., W. Fritz, and E. U. Schlunder, "Competitive Adsorption of Two Dissolved Organics onto Activated Carbon," *Chem. Eng. Sci.*, **36**, 743 (1981).

Perona, J. J., "Model for Sr-Cs-Ca-Mg-Na Ion Exchange Equilibria on Chabazite," *AIChE J.*, **39**, 1716 (1993).

Robinson, S. M., and J. M. Begovich, "Treatment Studies at the Process Waste Treatment Plant at Oak Ridge National Laboratory," ORNL/TM-10352, Oak Ridge National Laboratory, Oak Ridge, TN (1991).

Robinson, S. M., W. D. Arnold, and C. H. Byers, "Mass-Transfer Mechanisms for Zeolite Ion Exchange in Wastewater Treatment," *AIChE J.*, **40**(12), 2045 (1994).

Ruthven, D. M., *Principles of Adsorption and Adsorption Processes*, Wiley, New York (1984).

Smith, E. H., and W. J. Weber, Jr., "Modeling Activated Carbon Adsorption of Target Organic Compounds from Leachate-Contaminated Groundwaters," *Environ. Sci. Technol.*, **22**(3), 313 (1988).

Weber, W. J., Jr., and C. K. Wang, "A Microscale System for Estimation of Model Parameters for Fixed Bed Adsorbers," *Environ. Sci. Technol.*, **21**(11), 1096 (1987).

Yao, C., and C. Tien, "Approximations of Uptake Rate of Spherical Adsorbent Pellets and their Application to Batch Adsorption Calculations," *Chem. Eng. Sci.*, **48**(1), 187 (1993).

Manuscript received Apr. 1, 1996, and revision received June 6, 1996.